JOURNAL OF MATERIALS SCIENCE 28 (1993) 379–383

Formation, thermal stability and mechanical properties of amorphous alloys in the Mg–transition metal(Ni, Cu)–alkaline-earth metal(Ca, Sr, Ba) system

TOSHISUKE SHIBATA*, AKIHISA INOUE, TSUYOSHI MASUMOTO
Institute for Materials Research, Tohoku University, Sendai 980, Japan

Mg–Ni–Ca, Mg–Ni–Sr, Mg–Ni–Ba and Mg–Cu–Ca alloys were found to be amorphized by melt-spinning in the compositional ranges 0 to 30% Ni and 0 to 40% Ca, 5 to 20% Ni and 0 to 15% Sr, 10 to 25% Ni and 0 to 15% Ba, and 0 to 50% Cu and 0 to 35% Ca, respectively. In the amorphous Mg–Ni–Ca and Mg–Cu–Ca alloys, the glass transition was observed in the ranges of 7.5 to 15% Ni and 2.5 to 5% Ca and 10 to 40% Cu and 2.5 to 7.5% Ca, respectively. The crystallization temperature (T_x) of amorphous Mg–Cu–Ca alloys increases with increasing Cu content, while T_x for amorphous Mg–Ni–Ca and Mg–Ni–Sr alloys shows a maximum value of 459 and 471 K, respectively, at 15% Ni. The glass transition temperature (T_g) increases monotonously with increasing Ni or Cu content. Amorphous Mg–Ni–Ca and Mg–Ni–Sr ribbons containing more than 80% Mg have a good bending ductility and the highest tensile fracture strength (σ_f) reaches 690 and 680 MPa, respectively. The ratios of σ_f to density are nearly equal to those for previously reported Mg–Ni–(Y or Ln) amorphous alloys with higher σ_f values because of the low densities of the present Mg-based alloys.

1. Introduction

For the last four decades, a number of studies on rapidly solidified Mg alloys have been carried out [1] with the aim of clarifying the effect of melt-quenching on the microstructure and physical and chemical properties. As a result, the formation of an amorphous phase has been reported in rapidly solidified Mg–Zn [2], Mg–Cu [3] and Mg–Ni [3] alloys. Recently, Inoue *et al.* have found that Mg–Ni–Ln [4, 5], Mg–Cu–Ln (Ln = lanthanide metal), Mg–Ni–Y and Mg–Cu–Y [6] ternary alloys can be easily amorphized by the melt-spinning technique and the resulting amorphous alloys exhibit high mechanical strength, good ductility and a wide supercooled liquid region reaching about 60 K. The new amorphous alloys have also attracted considerable interest because of an expectation of subsequent development as a new type of high-strength material with light weight. However, little has been known about the glass formation of Mg–TM–AM (TM = transition metal, AM = alkaline earth metal) alloys and their thermal and mechanical properties. Most recently, the present authors have found that an amorphous single phase is formed in wide composition ranges in melt-spun Mg–Ni–AM and Mg–Cu–AM alloys. This paper is intended to clarify the glass formation range in melt-spun Mg–Ni–Ca, Mg–Ni–Sr, Mg–Ni–Ba and Mg–Cu–Ca ternary alloys and the thermal stability and mechanical strengths of their amorphous alloys.

2. Experimental procedure

Mg–TM–AM (TM = Ni or Cu, AM = Ca, Sr or Ba) ternary alloys were used in the present study. Their ingots were prepared by induction-melting mixtures of pure Mg (99.99 wt%), Ni (99.99 wt%), Cu (99.9 wt%) and AM (99 wt%) metals in an argon atmosphere. The compositions are nominally expressed in atomic per cent, since the weight loss of the pre-alloyed ingots is usually below 1%. From their master alloy ingots, ribbons with a cross-section of 0.02 mm × 1 mm were prepared in an argon atmosphere using a single roller melt-spinning equipment. The roller was made from Cu and its diameter was about 170 mm. The rotation speed of the roller was fixed at 66.7 s^{-1}. The amorphous nature of the melt-spun ribbons and the glass transition and crystallization behaviour of the amorphous phase were examined by X-ray diffractometry using CuK_α radiation, transmission electron microscopy (TEM) and differential scanning calorimetry (DSC). The heating rate in the DSC measurements was 0.67 K s^{-1} (40 K min^{-1}). Ductility was evaluated by a simple bending test. The term "ductile" implies that the ribbon can be bent through

* On leave from Yoshida Kogyo K.K., Yoshida Krobe Toyama Pref. 938, Japan.

0022–2461

180° without fracture. Hardness and tensile strength of the ribbon specimens were measured by a Vickers hardness tester with a 0.098 N load and an Instron-type tensile testing machine at a strain rate of $5.6 \times 10^{-4}\ s^{-1}$, respectively.

3. Results and discussion

3.1. Compositional ranges for formation of an amorphous phase

Figs 1–4 show the compositional ranges in which an amorphous phase is formed in melt-spun Mg–Ni–Ca, Mg–Cu–Ca, Mg–Ni–Sr and Mg–Ni–Ba alloys, respectively. The glass formation range in the Mg–Ni–Ca system shown in Fig. 1 extends widely from 0 to 30% Ni and 0 to 40% Ca, and binary Mg–Ca and Mg–Ni alloys are also amorphized around 10% Ca and in the range of 15 to 20% Ni. Furthermore, the glass transition phenomenon is observed in the range from 7.5 to 15% Ni and 2.5 to 5% Ca. Similarly, glass formation in the Mg–Cu–Ca system extends from 0 to 50% Cu and 0 to 35% Ca, and the glass transition is observed at 10 to 40% Cu and 2.5 to 7.5% Ca. The maximum value of the temperature interval between the glass transition temperature (T_g) and the crystallization temperature (T_x), $\Delta T_x (= T_x - T_g)$ is about 20 K for the Mg–Ni–Ca and Mg–Cu–Ca systems as shown in Fig. 5. The formation of the amorphous phase in Mg–Ni–Sr and Mg–Ni–Ba systems is limited to narrow ranges of 5 to 20% Ni and 0 to 15% Sr, and 10 to 25% Ni and 0 to 15% Ba, respectively. Thus, the glass-formation range is widest for the Mg–Cu–Ca system, followed by Mg–Ni–Ca, Mg–Ni–Sr and Mg–Ni–Ba systems.

The variation of the glass formation range seems to have a close relation to the negative enthalpy of mixing (ΔH_{mix}) among the constituent elements. The ΔH_{mix} value of the AM elements into Mg solvent has been calculated [7] to be -26 kJ g-at^{-1} for Ca, -19 kJ g-at^{-1} for Sr and -18 kJ g-at^{-1} for Ba. Similarly, the ΔH_{mix} value into Ni solvent is -37 kJ g-at^{-1} for Ca, -6 kJ g-at^{-1} for Sr and $+1$ kJ g-at^{-1}

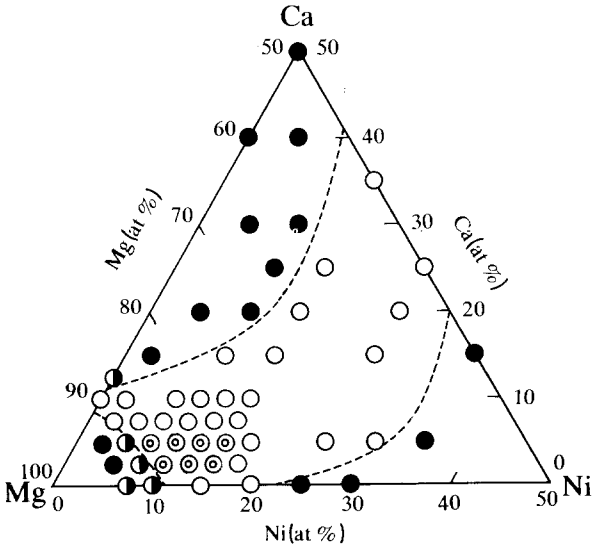

Figure 1 Composition for formation of an amorphous phase in Mg–Ni–Ca alloys: (◎) amorphous with T_g, (○) amorphous, (◑) amorphous + crystalline (●) crystalline.

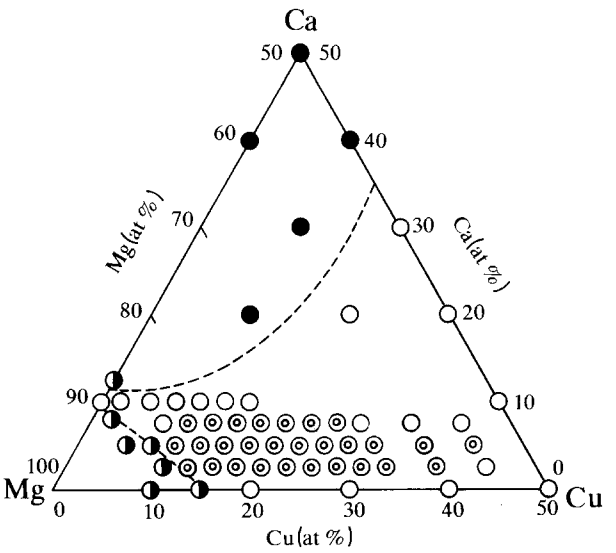

Figure 2 Composition range for formation of an amorphous phase in Mg–Cu–Ca alloys: (◎) amorphous with T_g, (○) amorphous, (◑) amorphous + crystalline (●) crystalline.

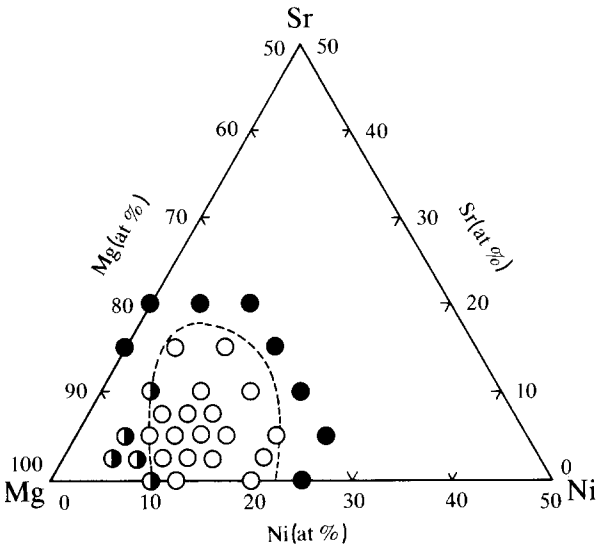

Figure 3 Composition range for formation of an amorphous phase in Mg–Ni–Sr alloys: (○) amorphous, (◑) amorphous + crystalline, (●) crystalline.

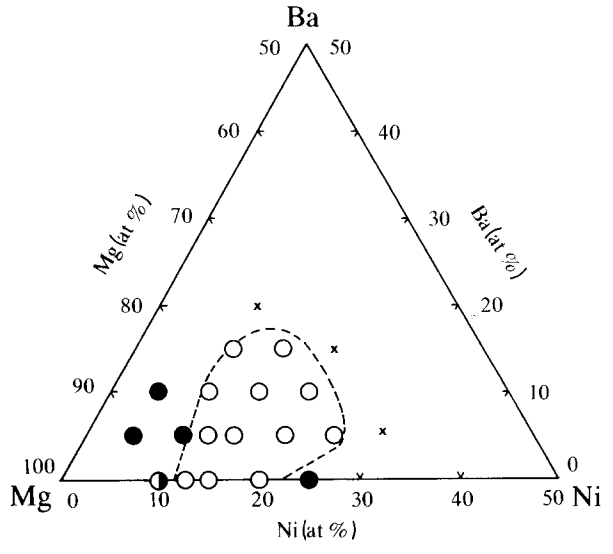

Figure 4 Composition range for formation of an amorphous phase in Mg–Ni–Ba alloys: (○) amorphous, (◑) amorphous + crystalline, (●) crystalline. The composition marked with x represents the fact that the preparation of pre-alloyed ingot is impossible.

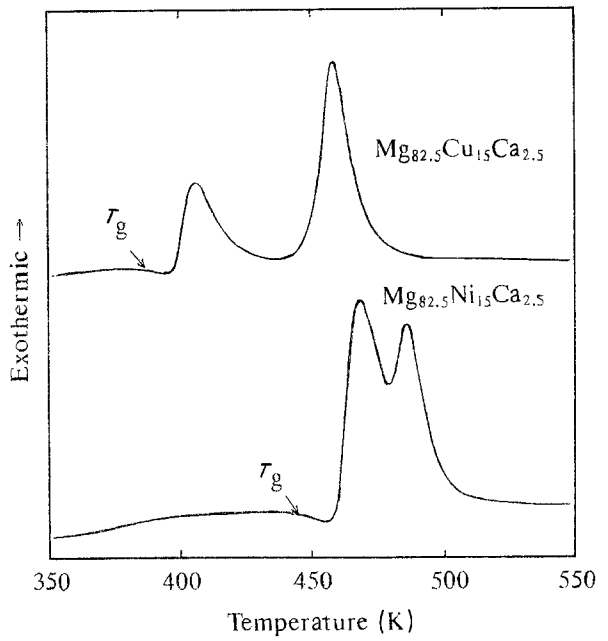

Figure 5 DSC curves of amorphous $Mg_{82.5}Cu_{15}Ca_{2.5}$ and $Mg_{82.5}Ni_{15}Ca_{2.5}$ alloys. Scanning rate 0.67 K s^{-1}.

for Ba. In addition, the ΔH_{mix} value into Mg solvent is -12 kJ g-at^{-1} for Ni and -29 kJ g-at^{-1} for Cu and that of Ca into Cu solvent is -103 kJ g-at^{-1}. Thus, the significant differences in their glass-formation ranges are presumed to result from differences of ΔH_{mix}. That is, there is a tendency that the larger the negative magnitude of ΔH_{mix} the wider is the glass-formation range.

In addition, the atomic size ratio is also thought to have a significant role in the glass-formation tendency. It is generally known that an amorphous phase tends to form in alloy systems consisting of elements with atomic size ratios exceeding about 10%. It is thought that a smaller atom occupies the gap constituted by larger atoms, leading to the formation of an amorphous phase with a higher degree of dense random packing. The atomic size ratio in the present Mg-based amorphous alloys is as large as 1.23 for Ca/Mg, 1.34 for Sr/Mg, 1.36 for Ba/Mg, 1.28 for Mg/Ni and 1.25 for Mg/Cu [8]. These results allow us to conclude that a wider glass-forming range is obtained in the combination among the elements whose average atomic size ratio is 1.23. When the atomic size ratio of constituent elements is about 1.2, one of the expected intermetallic compounds is an AB_2-type Laves phase. This is because the atomic size ratio plays a dominant role in the phase stability even in an equilibrium state, and the most dense packing state in AB_2 is obtained at an atomic size ratio of 1.225 [9]. The limitation of the glass-formation range suggests also that a higher degree of metastability is obtained at a limited atomic size ratio.

3.2. Thermal stability

Figs 6 and 7 show the compositional dependence of T_g for amorphous Mg–Ni–Ca and Mg–Cu–Ca alloys, respectively. T_g increases significantly with increasing Ni or Cu content, while there is no distinct tendency in the change of T_g with Ca content.

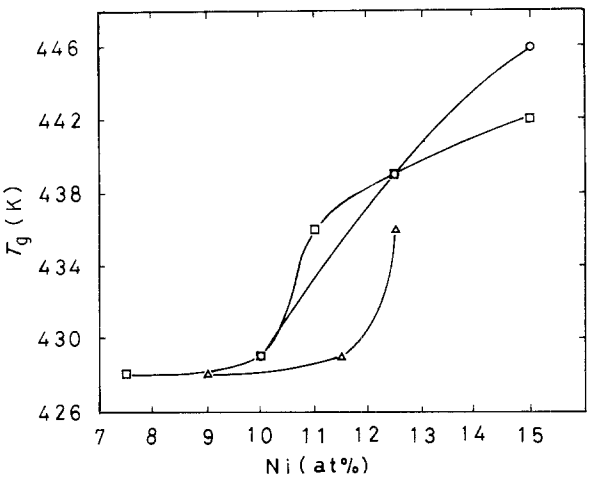

Figure 6 Compositional dependence of T_g for amorphous Mg–Ni–Ca alloys: Ca content (○) 2.5%, (△) 4%, (□) 5%.

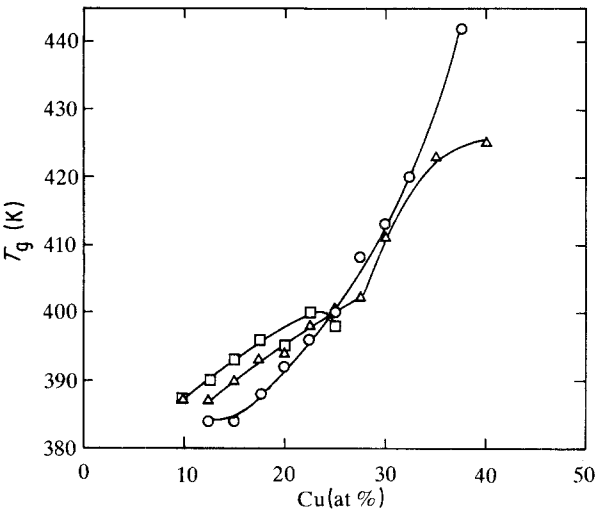

Figure 7 Compositional dependence of T_g for amorphous Mg–Cu–Ca alloys: Ca content (○) 2.5%, (△) 5%, (□) 7.5%.

Fig. 8 shows the compositional dependence of T_x for the Mg–Cu–Ca amorphous alloys. T_x increases monotonously with increasing Cu content, while the increase of T_x tends to decrease with increasing Ca content. This tendency appears to reflect the slope of the liquidus curve in each binary equilibrium phase diagram [10].

Figs 9 and 10 show the compositional dependence of T_x in amorphous Mg–Ni–Ca and Mg–Ni–Sr alloys, respectively. In the Mg–Ni–Ca system, T_x decreases with increasing Ca content. T_x as a function of Ni content shows a maximum of 459 K at 15% Ni, followed by a minimum at about 22.5% Ni and then a significant increase. The Mg–Ni–Sr amorphous alloy also shows a similar compositional dependence on Ni content and the maximum T_x value is obtained in the Ni concentration range 10 to 15%.

In order to investigate the reason for the appearance of the maximum T_x value, we examined the crystallization behaviour of the Mg–Ni–Ca amorphous alloys. In the range less than 15% Ni, the first-stage crystallization occurs through the simultaneous precipitation of Mg and an unknown compound as shown in Fig. 11. The unknown phase disappears

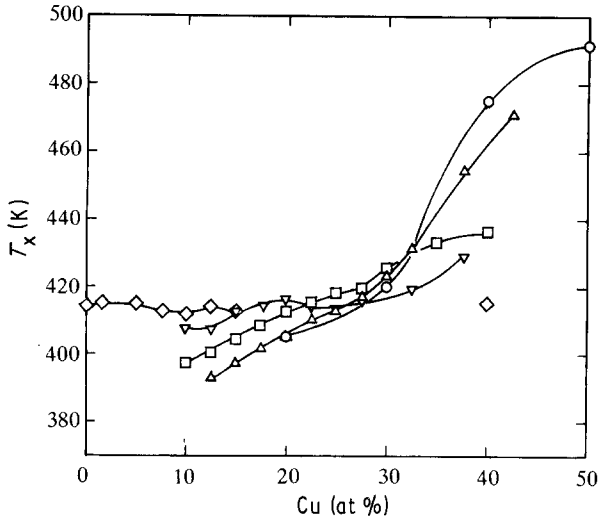

Figure 8 Compositional dependence of T_x for amorphous Mg–Cu–Ca alloys: Ca content (○) 0%, (△) 2.5%, (□) 5%, (▽) 7.5%, (◇) 10%.

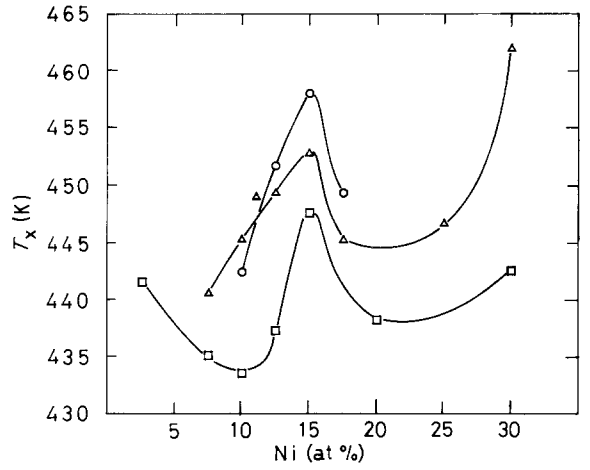

Figure 9 Compositional dependence of T_x for amorphous Mg–Ni–Ca alloys: Ca content (○) 2.5%, (△) 5%, (□) 10%.

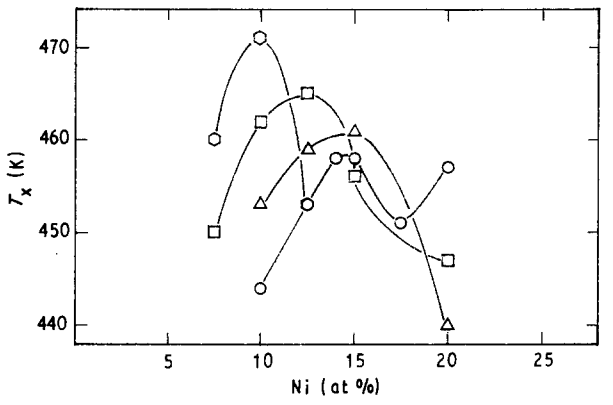

Figure 10 Compositional dependence of T_x for amorphous Mg–Ni–Sr alloys: Sr content (○) 1%, (△) 2.5%, (□) 5%, (◯) 7.5%.

completely in the Ni range above 15 at %. This result indicates that the crystallization process changes significantly in the vicinity of 15% Ni. Considering that a phase with the same diffraction peaks as the unknown phase is also observed in a binary Mg–Ni system and exists up to the melting temperature, the

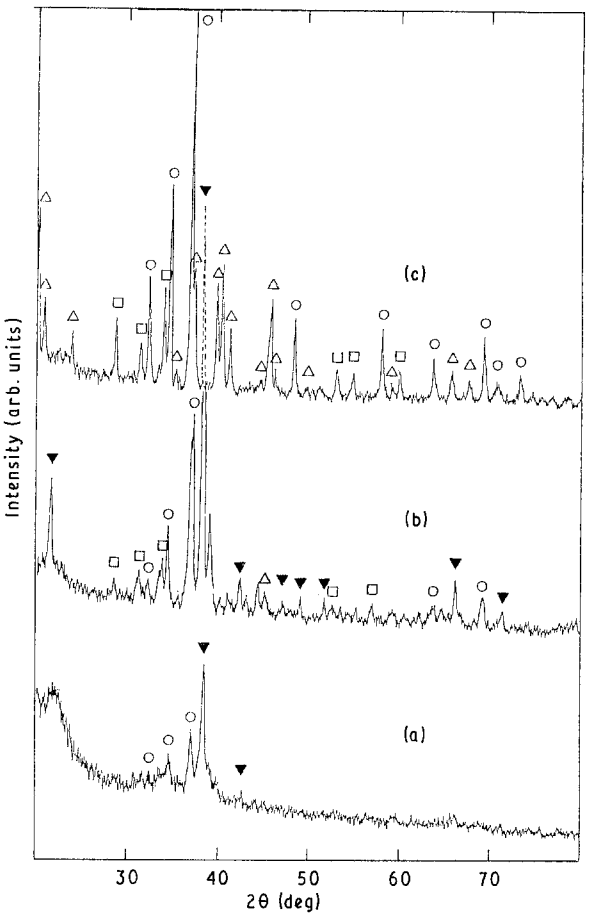

Figure 11 Change in the X-ray diffraction pattern of an amorphous $Mg_{85}Ni_{10}Ca_5$ alloy with annealing temperature: (a) 478 K, (b) 523 K, (c) 736 K, (○) Mg, (△) Mg_2Ni, (□) $CaMg_2$, (▼) X (unknown phase).

unknown phase seems to consist mainly of Mg and Ni elements.

3.3. Mechanical properties

Fig. 12 shows the compositional dependence of Vickers hardness (H_V) of amorphous Mg–Ni–Ca alloys. H_V increases monotonously with increasing Ni content and reaches a maximum value of 239 at 17.5% Ni. The amorphous Mg–Ni–Ca and Mg–Ni–Sr ribbons can be bent through 180° without fracture in the Mg-rich side. Table I summarizes the mechanical properties of some Mg–Ni–Ca and Mg–Ni–Sr amorphous alloys. The highest tensile fracture strength (σ_f) is 690 MPa for the Mg–Ni–Ca alloys and 680 MPa for the Mg–Ni–Sr alloys. These values are lower than the highest value (850 MPa) for amorphous Mg–Ni–Y [6] and Mg–Ni–Ln [4, 5] alloys, but the ratios of tensile strength to density for the present Mg-based alloys are nearly the same as for the Mg–Ni–Y and Mg–Ni–Ln alloys because of the low densities of the Mg–Ni–AM alloys.

It was mentioned above that the Mg–Ni–AM amorphous phase crystallized to mixed phases containing an unknown intermetallic compound. Consequently, the amorphous structure seems to have a particular atomic configuration reflecting the unknown compound which does not appear in any of the binary

TABLE I Mechanical properties of Mg–Ni–Ca and Mg–Ni–Sr amorphous alloys: density (d), Vickers hardness (H_v), tensile fracture strength (σ_f), tensile fracture strain (ε_f), Young's modulus (E), and the ratio of σ_f to density (σ_f/d)

Alloy	d (Mg m^{-3})	H_v	σ_f (MPa)	ε_f (%)	E (GPa)	σ_f/d (10^5 Nm kg^{-1})
$Mg_{90}Ni_{7.5}Ca_{2.5}$	1.99	182	610	1.5	40	3.1
$Mg_{82.5}Ni_{15}Ca_{2.5}$	2.27	239	690	1.4	49	3.1
$Mg_{84}Ni_{12.5}Ca_{3.5}$	2.16	219	520	1.2	44	2.4
$Mg_{84.5}Ni_{11.5}Ca_4$	2.12	196	570	1.5	38	2.7
$Mg_{87.5}Ni_{7.5}Ca_5$	1.97	176	650	1.4	47	3.3
$Mg_{89}Ni_{10}Sr_1$	2.11	167	530	1.4	38	2.5
$Mg_{84}Ni_{15}Sr_1$	2.30	215	680	1.7	40	3.0
$Mg_{85}Ni_{12.5}Sr_{2.5}$	2.23	185	560	1.5	37	2.5
$Mg_{82.5}Ni_{15}Sr_{2.5}$	2.32	216	380	1.0	38	1.7

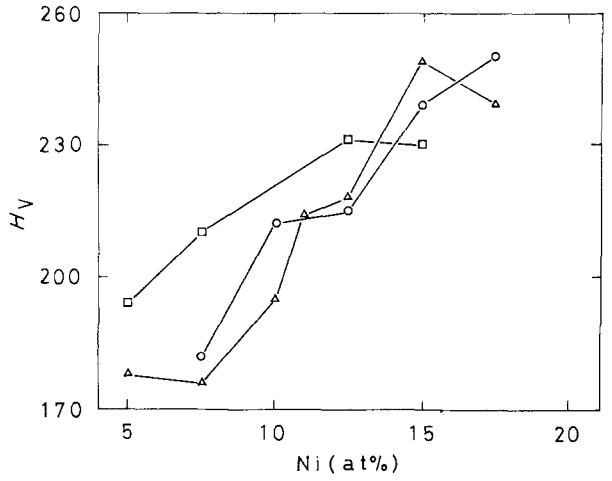

Figure 12 Compositional dependence of H_v for amorphous Mg–Ni–Ca alloys with good bending ductility. Ca content (○) 2.5%, (△) 5%, (□) 7.5%.

equilibrium phase diagrams. The peculiar atomic configuration also implies the existence of short-range ordering with a strong bonding nature which results in the high values of T_x, σ_f and H_v.

4. Summary

Amorphous Mg–Ni–Ca, Mg–Ni–Sr, Mg–Ni–Ba and Mg–Cu–Ca alloys form in the composition ranges of 0 to 30% Ni and 0 to 40% Ca, 5 to 20% Ni and 0 to 15% Sr, 10 to 25% Ni and 0 to 15% Ba, and 0 to 50% Cu and 0 to 35% Ca, respectively. In the Mg–Ni–Ca and Mg–Cu–Ca alloys, the glass transition phenomenon is observed in the ranges of 7.5 to 15% Ni and 2.5 to 5% Ca, and 10 to 40% Cu and 2.5 to 7.5% Ca, respectively, though the maximum value of $\Delta T_x (= T_x - T_g)$ is about 20 K for both the alloys. T_x increases monotonously with increasing Cu content in amorphous Mg–Cu–Ca alloys, while the T_x of amorphous Mg–Ni–Ca and Mg–Ni–Sr alloys shows a maximum value of 460 and 470 K, respectively, at 15% Ni.

In the range below 15% Ni, the first-stage crystallization occurs through the simultaneous precipitation of Mg and an unknown intermetallic compound. T_g increases monotonously with increasing Ni or Cu content in amorphous Mg–Ni–Ca and Mg–Cu–Ca alloys. Amorphous Mg–Ni–Ca and Mg–Ni–Sr ribbons containing above 80% Mg have a good bending ductility and the highest σ_f reaches 690 and 680 MPa, respectively. The ratio of σ_f to density for the present Mg-based alloys is nearly the same as for the amorphous Mg–Ni–Y and Mg–Ni–Ln alloys with higher σ_f values because of the low densities of the Mg–Ni–(Ca or Sr) alloys. Considering that amorphous alloys with the unknown compound as the primary precipitate exhibit maxima of T_x, σ_f and H_v, the peculiar atomic configuration reflecting the unknown compound suggests the existence of short-range ordering with a strong bonding nature.

References

1. R. S. BUSK and T. E. LEONTIS, *Trans. AIME* **188** (1950) 297.
2. A. CALKA, M. MADHARA, D. E. POLK, B. C. GIESSEN, H. MATYJA and J. VANDERSANDE, *Scripta Metall.* **11** (1977) 65.
3. F. SOMMER, G. BUCHER and B. PREDEL, *J. Phys. C* **8** (1980) 563.
4. A. INOUE, K. OHTERA, A. P. TSAI and T. MASUMOTO, *Jpn. J. Appl. Phys.* **27** (1988) L479.
5. A. INOUE, M. KOHINATA, A. P. TSAI and T. MASUMOTO, *Mater. Trans. JIM* **30** (1989) 378.
6. S. G. KIM, A. INOUE and T. MASUMOTO, *Mater. Trans.* **31** (1990) 929.
7. A. R. MEADEMA, F. R. de BOER and R. BOOM, *CALPHAD* **1** (1977) 341.
8. S. NAGASAKI, "Metals Databook" (1983) p. 8.
9. H. ABE, *Metallography* (1978) 113.
10. J. L. MURRAY, L. H. BENNET, H. BAKER and T. B. MASSALSKI, "Binary Alloy Phase Diagrams" (American Society for Metals, Ohio, 1986) p. 932.

Received 2 September 1991
and accepted 2 June 1992